

Glass transition temperature of freely-standing films of atactic poly(methyl methacrylate)

C.B. Roth and J.R. Dutcher^a

Department of Physics and the Guelph-Waterloo Physics Institute, University of Guelph, Guelph, Ontario, Canada N1G 2W1

Received January, 2003

Published online November 5, 2003 © EDP Sciences / Società Italiana di Fisica / Springer-Verlag 2003

Abstract. We have used ellipsometry to measure the glass transition temperature T_g of high molecular weight ($M_w = 790 \times 10^3$), freely-standing films of atactic poly(methyl methacrylate) (*a*-PMMA), as well as films of the same polymer supported on two different substrates: the native oxide layer of silicon (Si) and gold-covered Si. We observe linear reductions in T_g with decreasing film thickness h for the freely-standing PMMA films with $30 \text{ nm} < h < 100 \text{ nm}$, which is qualitatively similar to previous results obtained for freely-standing polystyrene (PS) films. However the magnitude of the T_g reductions for PMMA is much less than for freely-standing films of PS of comparable molecular weight and thickness. We also find that for films supported on either substrate, with thicknesses as small as 30 nm, the T_g values do not deviate substantially from the value measured for thick films.

PACS. 36.20.-r Macromolecules and polymer molecules – 64.70.Pf Glass transitions – 68.60.Bs Mechanical and acoustic properties of thin films

1 Introduction

Since the original measurements of reductions of the glass transition temperature T_g in thin polymer films supported on silicon [1], much work has been done to verify the results using other techniques, determine the effect of the free surfaces and the underlying substrate, and relate the glass transition temperature results to chain diffusion and segmental relaxation measurements [2,3]. Considerable progress in the understanding of the glass transition in thin polymer films has been achieved by studies of a simplified film geometry: freely-standing or unsupported films, for which there are no complicated polymer-substrate interactions and the film is symmetric about its midplane. Extensive measurements have been performed on freely-standing PS films, using Brillouin Light Scattering (BLS) for both high and low molecular weight (M_w) PS [4,5,6], and transmission ellipsometry for high M_w PS [7]. T_g reductions at small film thicknesses are observed for both high and low M_w PS freely-standing films. For low M_w values, $M_w < 350 \times 10^3$, $T_g(h)$ shows the same behavior as that observed for supported PS films, whereas for high M_w values, $M_w > 350 \times 10^3$, the T_g values decrease linearly with decreasing film thickness h , with the slope dT_g/dh increasing with increasing M_w .

A variety of different theoretical models have been proposed to describe the glass transition measurements for

both supported and freely-standing polymer films. The models use different approaches to interpret the effect of the polymer film interfaces on T_g , incorporating chain end segregation [8], mobile surface layers [6], surface fluctuation/capillary waves [9,10], surface mobility coupled with chain connectivity (“sliding mode”) [11], reduction in intermolecular coupling and reduced entanglement near surfaces [12,13], and percolation [14]. These models meet with varying degrees of success in explaining the various aspects of the body of data that has been collected for freely-standing and supported polymer films, with no one model able to describe quantitatively all of the data. In addition, none of the models accounts for chemical and steric differences between polymers, although these effects, *e.g.* steric hindrances, will have implications for enhanced surface mobility.

In the present study, we have measured the film thickness dependence of T_g of freely-standing films of another polymer, atactic poly(methyl methacrylate) (*a*-PMMA). Since the T_g value depends dramatically on tacticity for bulk PMMA [15] and supported PMMA films [16], we have chosen to measure $T_g(h)$ for atactic PMMA (*a*-PMMA) freely-standing films so that we can compare our results to those obtained previously for freely-standing atactic PS films [4,5,7]. In addition, the PMMA freely-standing film results are also compared to those obtained for similar PMMA films supported on two different substrates.

^a e-mail: dutcher@physics.uoguelph.ca

2 Experimental techniques

2.1 Sample preparation

Atactic PMMA (*a*-PMMA) [17] of high molecular weight ($\overline{M}_w = 790 \times 10^3$; root-mean-square end-to-end distance $R_{ee} = 60$ nm [18]) and narrow distribution ($\overline{M}_w/\overline{M}_n = 1.10$) was dissolved in toluene. Thin films of PMMA were deposited by spincoating dilute solutions (solution concentrations between 1.0% and 3.46% PMMA by mass; spin speeds between 1500 and 5000 rpm) onto freshly-cleaved mica, silicon wafers with a thin native silicon oxide (SiO_x) layer, and gold-covered silicon oxide (gold evaporated at a rate of 20 nm/s with a thickness of approximately 200 nm and root-mean-square (rms) roughness of approximately 15 nm, as measured using atomic force microscopy). Films with thicknesses between 30 nm and 308 nm were used in the present study. The PMMA films on the various substrates were annealed under vacuum at $T = 125$ °C for 12 h to remove residual solvent and cooled at 1 °C/min to room temperature. Freely-standing PMMA films were fabricated by using a water transfer technique [5] to transfer the PMMA films from the mica substrates onto 1 cm² nylon sample holders containing 4 mm or 5 mm diameter holes. Nylon sample holders were used to suspend the freely-standing films as this was found to reduce the stress produced in the polymer with changes in temperature due to differential thermal expansion between the sample and holder [7]. Pieces of the same PMMA films were also transferred onto clean Si wafers for a determination of the initial PMMA film thickness, accurate to within ± 1 nm, using ellipsometry.

2.2 Experiment description and procedures

The dependence of the film thickness and index of refraction of the PMMA films was measured using ellipsometry. The ellipsometry measurements were performed using our custom-built, single-wavelength ($\lambda = 632.8$ nm), self-nulling ellipsometer in transmission mode for the freely-standing films and in reflection mode for the supported films. Relative measurements of the ellipsometry angles P and A required to obtain a null in the intensity at the detector are accurate to within $\pm 0.001^\circ$. For further details on measurements performed using our custom-built ellipsometer, the reader is referred to [7].

Reflection ellipsometry measurements were performed at an angle of incidence of $\theta_i = 40^\circ$ and transmission ellipsometry measurements were performed for θ_i approximately equal to the Brewster angle of PMMA, $\theta_B = 56^\circ$. At the beginning of each ellipsometry experiment, the temperature was increased rapidly at a rate of 5 °C/min from room temperature to a temperature $T = 110$ °C. At the elevated temperature, the sample chamber was then flushed with approximately 30 liters of room temperature dry nitrogen gas, with both sides of the freely-standing film exposed to the nitrogen gas, for typically 30 s to remove any water vapour in the chamber, since water acts as a plasticizer to PMMA which reduces the T_g value [19].

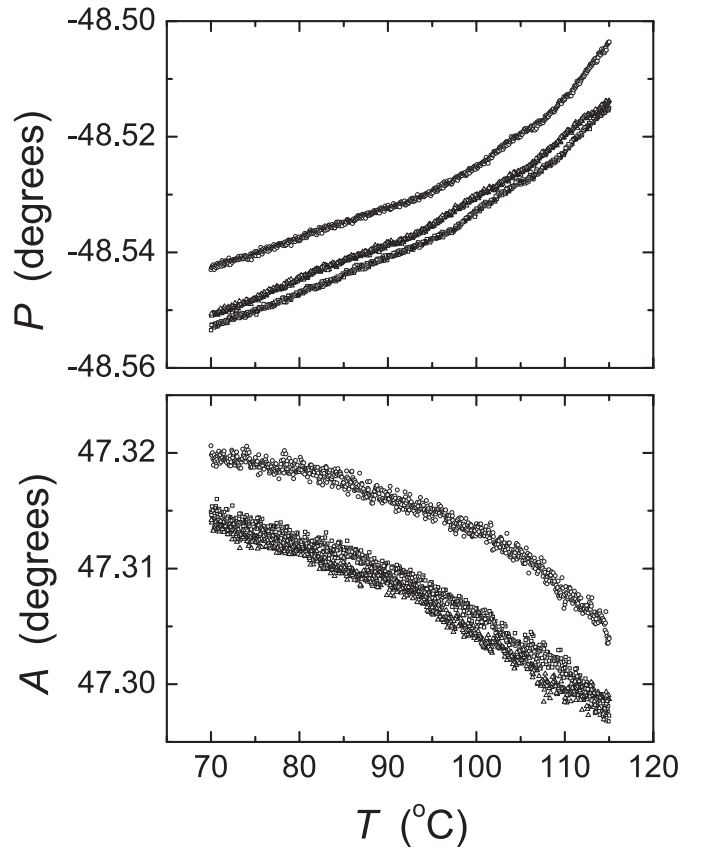


Fig. 1. Ellipsometry angles P and A versus temperature T of a freely-standing *a*-PMMA film with thickness $h = 40$ nm for the initial cooling from $T = 115$ °C, and subsequent heating and cooling cycles. The data for the heating cycle is shown with open circles and has been shifted to slightly larger P ($+0.01^\circ$) and A ($+0.005^\circ$) values for clarity.

Following the gas flushing, the temperature was allowed to equilibrate for 10 minutes and then the temperature was increased to a temperature that was at least 20 °C greater than T_g to allow the measurement of T_g upon cooling. Nitrogen gas flushing was not performed during the ellipsometry measurements because gas flow caused vibrations of the freely-standing films.

Measurements of P and A were collected as the temperature was decreased and increased at a rate of 0.5 °C/min through the glass transition temperature. Typically 3 to 5 thermal (heating and cooling) cycles were performed for each film, and the range of temperatures T was 60 °C $< T < 120$ °C for freely-standing films and 90 °C $< T < 140$ °C for supported films. In Figure 1 are shown the P and A values as a function of temperature T for three temperature ramps of a freely-standing PMMA film with a room temperature thickness of $h = 40$ nm. As in previous work [7], we have converted the P and A values at each temperature to the film thickness h and index of refraction n by assuming an isotropic index of refraction [20] (see Fig. 2). For PMMA films supported on the native oxide layer of silicon wafers, we used a model incorporating two layers on a semi-infinite

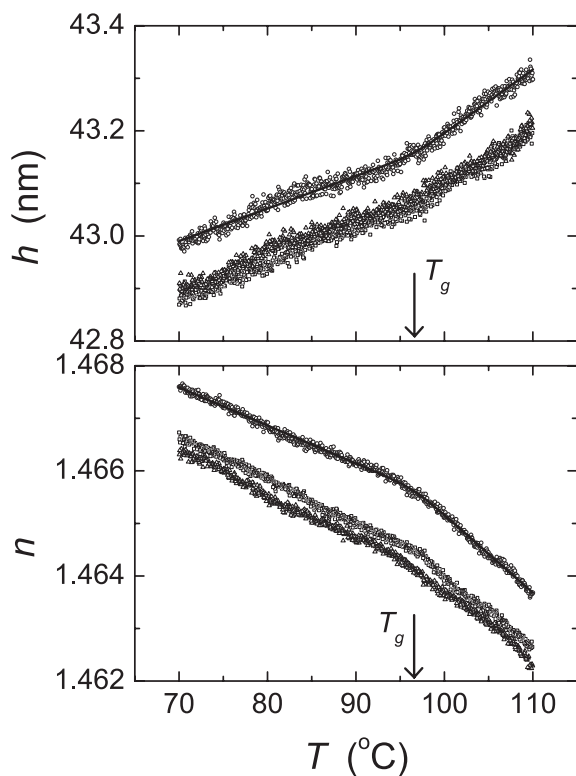


Fig. 2. Film thickness h and index of refraction n versus temperature T obtained by fitting the $P(T)$ and $A(T)$ shown in Figure 1 for a freely-standing a -PMMA film. As in Figure 1, the data for the heating cycle is shown with open circles and has been shifted to slightly larger h (+0.1 nm) and n (+0.001) values for clarity. The solid lines correspond to fits of the data obtained on the heating cycle to equation 1, and the vertical arrows correspond to the best fit values of T_g .

substrate (PMMA/SiO_x/Si). The index of refraction of the SiO_x layer was taken to be $n(\text{SiO}_x) = 1.4598$ [21] and the thickness of the SiO_x layer was measured to be $h(\text{SiO}_x) = 2$ nm from ellipsometry measurements of bare silicon wafers with the native SiO_x layer. The complex index of refraction of the Si substrate was taken to be $3.8858 - 0.02i$ at the laser wavelength ($\lambda = 632.8$ nm) [22]. For the gold-covered Si wafers, the 200 nm thick layer of gold can be taken to be a semi-infinite substrate for the purposes of the ellipsometry analysis. However, we found that the ellipsometry measurements of P and A for the gold-covered Si wafers did not yield reasonable values of the index of gold (possibly due to the large rms roughness of the gold films), and the raw $P(T)$ and $A(T)$ data were used to determine the T_g value instead.

To obtain the T_g value for each heating and cooling cycle, the h and n data were fit to a function of the form

$$w_i \left(\frac{M_i - G_i}{2} \right) \ln \left(\cosh \left(\frac{T - T_g}{w_i} \right) \right) + (T - T_g) \left(\frac{M_i - G_i}{2} \right) + c_i, \quad i = h, n. \quad (1)$$

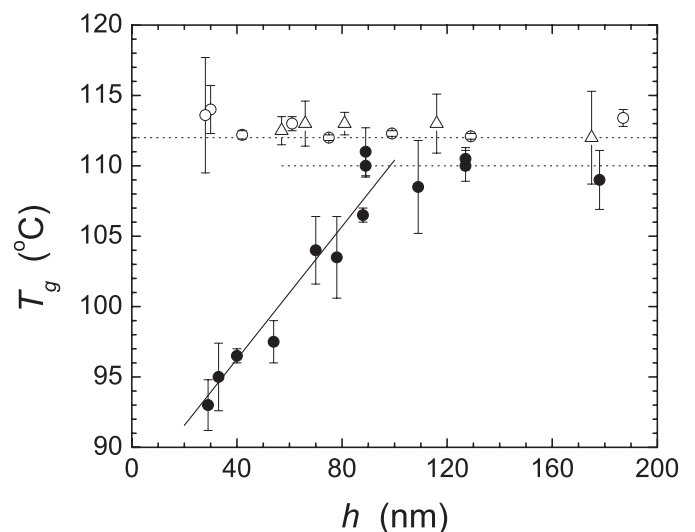


Fig. 3. T_g versus h for the three different types of a -PMMA films ($M_w = 790 \times 10^3$) used in the present study: freely-standing (solid circles), supported on native oxide/silicon (open circles), and supported on Au/native oxide/silicon (open triangles). The solid straight line corresponds to the best linear fit to the freely-standing film data for $h < 100$ nm, the horizontal dashed lines correspond to the average of the T_g values measured for the thickest freely-standing films, and the upper horizontal dashed line corresponds to the T_g value ($T_g = 112$ °C) measured for a very thick ($h = 308$ nm) PMMA film supported on the native oxide layer of silicon.

Equation (1) is an empirical equation we have used previously to fit freely-standing PS ellipsometry data [7], that is derived by integrating an assumed $\tanh(T)$ profile for the transition between thermal expansion coefficients in the glass and melt. In equation (1) M_i and G_i are the dh/dT and dn/dT slope values of the melt and glass respectively, w_i is the width of the transition, and c_i is the value of the film thickness or index of refraction at $T = T_g$. This equation is used to determine T_g , instead of using the intersection of linear fits to the data above and below T_g , for both the $h(T)$ and $n(T)$ data, to avoid the subjectivity of choosing the range of temperatures corresponding to the linear regions in the data at temperatures above and below T_g . The width of the transition w_i was fixed at 2 °C which was found to provide excellent fits in all cases. For each temperature ramp, values of T_g were determined from a nonlinear least squares fit of equation (1) to both the $h(T)$ and $n(T)$ data. This procedure was carried out for several thermal cycles and the T_g value of the film was calculated as the average value of all measured T_g values. We observed no systematic differences between T_g values obtained on successive temperature ramps.

3 Results and discussion

In Figure 3 are shown the $T_g(h)$ data collected for the three different PMMA film geometries used in this study: freely-standing (solid circles), supported on native oxide layer of silicon (open circles) and supported

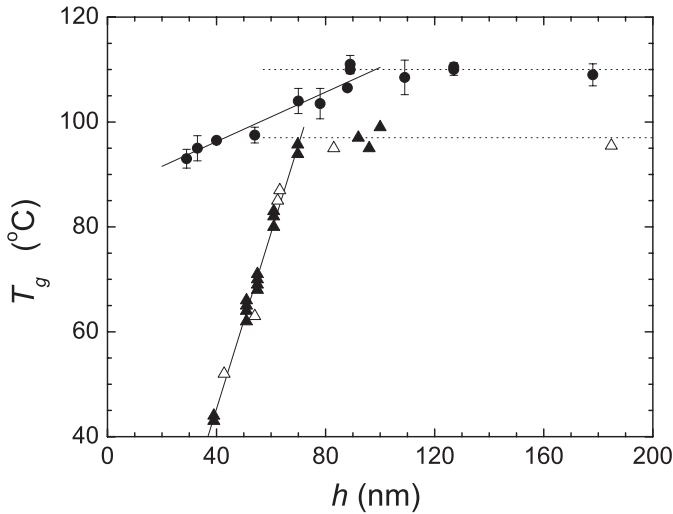


Fig. 4. T_g versus h for freely-standing α -PMMA and PS films of nearly identical molecular weights. The solid circles correspond to data collected using ellipsometry for α -PMMA ($M_w = 790 \times 10^3$), the solid triangles correspond to data collected using ellipsometry for PS ($M_w = 767 \times 10^3$) [7], and the open triangles correspond to data collected using Brillouin light scattering for PS ($M_w = 767 \times 10^3$) [7]. The solid straight lines correspond to the best linear fits to the data for $h < 100$ nm (α -PMMA) and $h < 70$ nm (PS), and the horizontal dashed lines correspond to the average of the T_g values measured for the thickest freely-standing films ($T_g = 110$ °C for α -PMMA and $T_g = 97$ °C for PS).

on gold-covered substrates (open triangles). T_g decreases linearly with decreasing film thickness for the PMMA freely-standing films below a threshold film thickness value (≈ 100 nm), which is qualitatively similar to the $T_g(h)$ behavior observed previously for freely-standing PS films [4,5,7]. For the range of film thicknesses used in the present study ($30 \text{ nm} < h < 308 \text{ nm}$), there is no substantial deviation of the measured T_g values, within the uncertainty of the measurements, from the T_g value measured at large film thicknesses for the PMMA films supported on both types of substrates. The results obtained for the supported films are similar to those of Grohens *et al.* [16] who found no substantial difference between the T_g values measured for α -PMMA films on silicon wafers and evaporated aluminum for film thicknesses between 35 and 40 nm. The lack of the film thickness dependence of T_g obtained for the α -PMMA films on SiO_x/Si substrates with $h > 30$ nm and on gold-covered substrates with $h > 60$ nm in the present study is also consistent with the results reported by Keddie *et al.* [23] for syndiotactic PMMA on similar substrates.

Despite the qualitative similarities between the results for the PMMA and PS freely-standing films, there are some important quantitative differences. In Figure 4 is shown a comparison of the $T_g(h)$ data obtained for the PMMA freely-standing films (with $\overline{M}_w = 790 \times 10^3$ and $R_{ee} = 60$ nm [18]) and the $T_g(h)$ data obtained previously using the same ellipsometer and the same experimental procedure for PS freely-standing films of com-

parable molecular weight ($\overline{M}_w = 767 \times 10^3$ and $R_{ee} = 64$ nm [18]) [4,5,7]. Clearly, the reductions in T_g are much larger for the PS films than for the PMMA films. This is true both for a given film thickness, or a given film thickness less than the threshold film thickness value below which T_g reductions are observed. In particular, the slope dT_g/dh is much larger for the PS films than for the PMMA films. The possibility of plasticization of PMMA by water is not likely the cause of the quantitative differences between the results obtained for PMMA and PS freely-standing films for two reasons: (1) the chamber of the sample cell was flushed with dry nitrogen gas at high temperature which should remove the water vapour from the sample cell, and (2) plasticization of PMMA would lead to larger T_g reductions for PMMA and therefore smaller differences between the $T_g(h)$ results for the two types of films.

As mentioned in the Introduction, the various models that have been proposed to explain aspects of the T_g results obtained on freely-standing and supported polymer films have not incorporated polymer-specific properties, *e.g.* chemical structure, steric hindrance. The present results indicate that such polymer-specific properties can have a considerable effect on T_g reductions in thin polymer films, and efforts to incorporate these effects into existing and new theoretical models are strongly encouraged.

4 Summary and conclusions

We have measured the glass transition temperature T_g in freely-standing and supported α -PMMA films of high molecular weight $M_w = 790\text{k}$ using transmission and reflection ellipsometry. T_g reductions with decreasing film thickness were observed for freely-standing PMMA films, whereas no substantial change in T_g with film thickness was observed for supported PMMA films with $30 \text{ nm} < h < 308 \text{ nm}$. The $T_g(h)$ behavior for the freely-standing PMMA films was qualitatively similar to that obtained previously for freely-standing PS films of the same tacticity, with a linear decrease in T_g with decreasing film thickness. However, the T_g reductions were much smaller for the PMMA freely-standing films than for the PS freely-standing films. These results demonstrate that the magnitude of T_g reductions in thin polymer films can vary greatly with the type of polymer, an effect that should be incorporated into theoretical models.

Financial support of the Natural Sciences and Engineering Research Council (NSERC) of Canada is gratefully acknowledged.

References

1. J.L. Keddie, R.A.L. Jones, R.A. Cory, *Europhys. Lett.* **27**, 59 (1994)
2. See, for example, *Eur. Phys. J. E* **8**, 99–266 (2002)

3. For a recent review, see J.A. Forrest, K. Dalnoki-Veress, Adv. Colloid Interface Sci. **94**, 167 (2001)
4. J.A. Forrest, K. Dalnoki-Veress, J.R. Stevens, J.R. Dutcher, Phys. Rev. Lett. **77**, 2002 (1996); **77**, 4108 (1996)
5. J.A. Forrest, K. Dalnoki-Veress, J.R. Dutcher, Phys. Rev. E **56**, 5705 (1997)
6. J.A. Forrest, J. Mattsson, Phys. Rev. E **61**, R53 (2000)
7. K. Dalnoki-Veress, J.A. Forrest, C. Murray, C. Gigault, J.R. Dutcher, Phys. Rev. E **63**, 031801 (2001)
8. A.M. Mayes, Macromolecules **27**, 3114 (1994)
9. S. Herminghaus, K. Jacobs, R. Seemann, Eur. Phys. J. E **5**, 531 (2001)
10. S. Herminghaus, Eur. Phys. J. E **8**, 237 (2002)
11. P.-G. de Gennes, Eur. Phys. J. E **2**, 201 (2000)
12. K. Ngai, Rizos, Mater. Res. Soc. Proc. **455**, 147 (1997)
13. K. Ngai, Eur. Phys. J. E **8**, 225 (2002)
14. D. Long, F. Lequeux, Eur. Phys. J. E **4**, 371 (2001)
15. *Physical Properties of Polymers Handbook*, ed. J.E. Mark (Springer-Verlag, New York, 1996)
16. Y. Grohens, M. Brogley, C. Labbe, M.-O. David, J. Schultz, Langmuir **14**, 2929 (1998)
17. Obtained from PSS Polymer Standards Service GmbH.
18. P.J. Flory, *Principles of Polymer Chemistry* (Cornell University Press, Ithaca, 1953)
19. L.S.A. Smith, V. Schmitz, Polymer **29**, 1871 (1988)
20. R.M.A. Azzam, N.M. Bashara, *Ellipsometry and Polarized Light* (North-Holland Publishing Company, Amsterdam, 1977)
21. Optrel GbR, Berlin, Germany
22. *Handbook of Optical Constants of Solids*, edited by E.D. Palik (Academic, Orlando, 1985)
23. J.L. Keddie, R.A.L. Jones, R.A. Cory, Faraday Discuss. **98**, 219 (1994)